Exact results and approximation schemes for the Schwinger Model with the Overlap Dirac Operator*

L. Giusti, C. Hoelbling, C. Rebbi

Boston University - Department of Physics, 590 Commonwealth Avenue, Boston MA 02215.

We propose new techniques to implement numerically the overlap-Dirac operator which exploit the physical properties of the underlying theory to avoid nested algorithms. We test these procedures in the two-dimensional Schwinger model and the results are very promising. We also present a detailed computation of the spectrum and chiral properties of the Schwinger Model in the overlap lattice formulation.

The overlap [1] formulation of lattice fermions provides a definition of a lattice Dirac operator D which avoids the doubling problem and preserves the relevant symmetries of the continuum theory, most notably chiral symmetry in the limit of vanishing fermion mass. Unfortunately, this welcome development has come at a price: the numerical calculation of the matrix elements of the propagator D^{-1} and the inclusion of $\mathrm{Det}(D)$ in the measure entail a substantially increased computational burden, which severely constrains the maximum lattice size for viable simulations. In this talk we present results of an exploratory study for a numerical approximation which exploits the physical properties of the system. It proceeds through the projection over a subspace which has a substantially reduced number of degrees of freedom but still captures the relevant non-perturbative long range properties of the model.

The Schwinger model is an ideal laboratory to test our approximation: it has many features in common with QCD, most notably chiral symmetry, and it is simple enough that it is possible to compute D^{-1} and $\mathrm{Det}(D)$ exactly within the overlap formulation. Our primary goal is to compare the results of our approximation to exact results. Nevertheless the results of the exact calculations are interesting per se, because they are more extensive than what, to the best of our knowledge, has been obtained up to now and validate in an impressive manner the advantages of Neuberger's formulation of lattice fermions. This talk is based on a work which will be the subject of a forthcoming publication [2], where all the notations used here and the details of the simulations are reported.

*The authors have been supported in part under DOE grant DE-FG02-91ER40676.

1. The Schwinger Model with Overlap Fermions

The Euclidean action of the Schwinger Model in the overlap regularization is given by

$$\begin{aligned} S_L &= \beta \sum_{x,\mu<\nu} [1 - \mathrm{Re}\, U_{\mu\nu}(x)] \\ &+ \sum_{i=1}^{N_f} \sum_{x,y} \bar{\psi}_i(x) \left[(1 - \frac{ma}{2}) D(x,y) + m \right] \psi_i(y) \end{aligned} \tag{1}$$

where $U_{\mu\nu}(x)$ is the standard Wilson plaquette, ψ_i are N_f fermions fields with mass m and $\beta = 1/(ag)^2$, g being the bare coupling constant. D is the massless overlap-Dirac operator

$$\begin{aligned} D &= \frac{1}{a}\left(1 + X\frac{1}{\sqrt{X^\dagger X}}\right) \\ X &= D_W - \frac{1}{a}\,, \end{aligned} \tag{2}$$

where D_W is the Wilson-Dirac operator and a is the lattice spacing. The Neuberger-Dirac operator satisfies the γ_5-Hermiticity condition

$$D^\dagger = \gamma_5 D \gamma_5 \tag{3}$$

and the Ginsparg-Wilson (GW) relation [3]

$$\gamma_5 D^{-1} + D^{-1}\gamma_5 = a\gamma_5 \tag{4}$$

The latter equation implies a continuous symmetry of the fermion action in Eq. (1) at finite lattice spacing [4]

$$\delta\psi = \hat{\gamma}_5\psi \qquad \delta\bar{\psi} = \bar{\psi}\gamma_5 \tag{5}$$

where $\hat{\gamma}_5 = \gamma_5(1-aD)$, which may be interpreted as a lattice form of the chiral symmetry. The chiral transformations in Eq. (5) lead to Ward identities analogous to the continuum ones and the anomaly term arises from the non-invariance of the fermion integral measure [4]. The corresponding flavor non-singlet chiral transformations are defined including a flavor group generator in Eq. (5). They imply the Axial Ward identities

$$\partial_\mu A^c_\mu = 2mP^c + O(a^2) \tag{6}$$

where the axial current and the pseudoscalar densities are

$$A^c_\mu = \bar{\psi}\frac{\lambda^c}{2}\gamma_\mu\gamma_5\psi \qquad P^c = \bar{\psi}\frac{\lambda^c}{2}\gamma_5\psi \tag{7}$$

with $\psi = (\psi_i, \ldots \psi_{N_f})$, and λ^c are the generators of the $SU(N_f)$ flavor group. In two dimensions the Axial current is related to the Vector one as

$$A^c_\mu(x) = -i\epsilon_{\mu\nu}V^c_\mu(x) \tag{8}$$

where $\epsilon_{\mu\nu}$ is the totally antisymmetric tensor.

In the $N_f = 2$ massless model, there is a triplet of massless particles (π) and one massive singlet particle (η) with mass $(M_\eta/g)^2 = 2/\pi$. The correlation functions of the vector currents are the same as for free particles. For small masses the corrections to the massless results can be obtained by "chiral perturbation" theory [5] which to first order gives

$$\begin{aligned} \frac{M_\pi}{g} &= e^{2\gamma/3}\frac{2^{5/6}}{\pi^{1/6}}\left(\frac{m}{g}\right)^{2/3} \\ \left(\frac{M_\eta}{g}\right)^2 &= \frac{2}{\pi} + \left(\frac{M_\pi}{g}\right)^2 \end{aligned} \tag{9}$$

where $\gamma = 0.577216\ldots$ is Euler's constant.

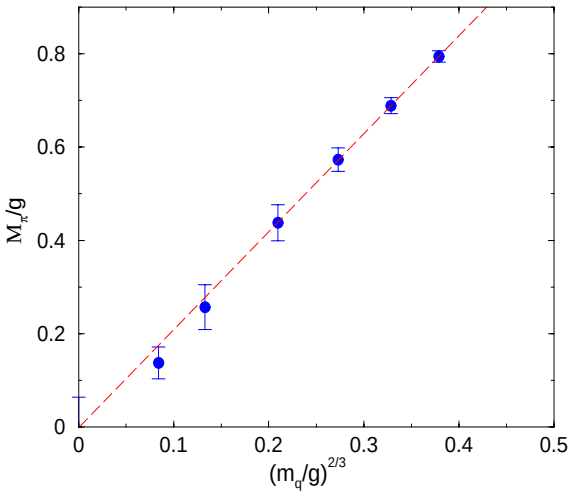

Figure 1. M_π/g vs $(m/g)^{2/3}$ for the full operator for $N_f = 2$.

2. Numerical results with the full operator

In order to test our approximation method and, at the same time, to increase the body of informations on the lattice Schwinger model, we performed an extensive simulation with the exact Neuberger-Dirac operator. We considered the Schwinger model at $\beta = 6$ on a 24×24 lattice. On a lattice of this size, the discretized Dirac operator is a complex matrix of dimension 1152×1152, for which we could use full matrix algebra subroutines without excessive burden on the resources available to us (Boston University SGI/Cray Origin 2000 supercomputer). The masses have been selected on the basis of previous results which indicated that, for most of the values we were planning to consider, the lattice would span at least a few correlation lengths. We generated 500 independent configurations of the gauge variables $U_\mu(x)$ distributed according to the pure gauge Wilson action of Eq. (1). For calculations with one and two flavors of dynamical fermions, we incorporated the determinant of the lattice Dirac operator in the averages of the correlation functions [6]. While with large variations of the determinant this way of proceeding would lead to an unacceptable variance, in the present calculation we found the range of values taken by $\mathrm{Det}(D)$ to

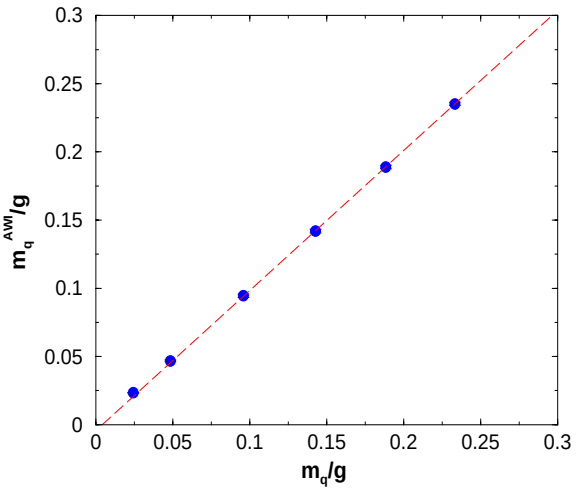

Figure 2. m^{AWI}/g vs m/g for the full operator for $N_f = 2$.

be sufficiently limited to warrant our averaging procedure (see Fig. 8).

For each configuration, we performed a singular value decomposition

$$D_W - \frac{1}{a} = U\Lambda\tilde{U} \tag{10}$$

where $U, \tilde{U}$ are unitary matrices and Λ is diagonal, real and non-negative. The operator $V = X/\sqrt{X^\dagger X}$ in Eq. 2 is then given by

$$V = U\tilde{U} \tag{11}$$

We proceeded then to the diagonalization of V, calculating all its eigenvalues and eigenvectors. From these, it is straightforward to calculate both the determinant of the Neuberger-Dirac operator D as well as its associated propagator D^{-1} for any value of the fermion mass m. The full diagonalization of V is computationally more demanding than the direct calculation of D^{-1}, which typically gives also Det(D) as a by-product, but we were interested in the actual spectrum of V for comparison with the approximations that will be discussed later. From the fermion propagators we calculated the meson propagators projected over zero momentum. We focused on the two point correlation functions of the singlet vector current

Table 1
Mesons and quark masses for $N_f = 2$.

$\beta = 6.0$, $V = 24^2$, $N_f = 2$			
m/g	m^{AWI}	m_π/g	m_η/g
Analytic			
0	0	0	0.7979
Full Operator			
0.00	-0.004(2)	-0.001(65)	1.00(25)
0.0244	0.0233(2)	0.14(3)	1.0(5)
0.0485	0.0468(6)	0.26(5)	1.0(4)
0.0960	0.0945(13)	0.44(4)	1.1(2)
0.1427	0.1420(14)	0.57(3)	1.1(2)
0.1884	0.1890(13)	0.69(2)	1.2(1)
0.2333	0.2353(11)	0.79(1)	1.23(9)
Fourier Approximation			
0.00	-0.002(2)	-0.005(66)	-
0.0244	0.018(1)	0.11(3)	-
0.0485	0.044(1)	0.24(5)	-
0.0960	0.092(1)	0.43(4)	-
0.1427	0.139(1)	0.57(3)	-
0.1884	0.184(1)	0.68(2)	-
0.2333	0.228(1)	0.79(1)	-
Multi-grid Determinant			
0.00	-0.004(1)	-0.002(40)	1.09(25)
0.0244	0.0234(1)	0.14(2)	1.1(4)
0.0485	0.0469(4)	0.26(3)	1.1(4)
0.0960	0.0946(9)	0.44(2)	1.1(2)
0.1427	0.1420(10)	0.57(2)	1.2(2)
0.1884	0.1889(9)	0.68(1)	1.2(1)
0.2333	0.2351(8)	0.79(1)	1.26(9)

and the triplet current

$$C_T(t) = \sum_{x,x',y} \langle V_2(x,y)V_2(x',y+t)\rangle \tag{12}$$

because they are saturated by a single particle contribution in the massless limit. We added to the averages the correlators obtained from the interchange of x and y in Eq. 12 for a further gain in statistics.

From fits to the meson correlators we extracted the meson masses in a standard manner. Our results for the meson and quark masses as functions of the fermion mass parameter of the action are reported in Figs. 1 and 2. The values we

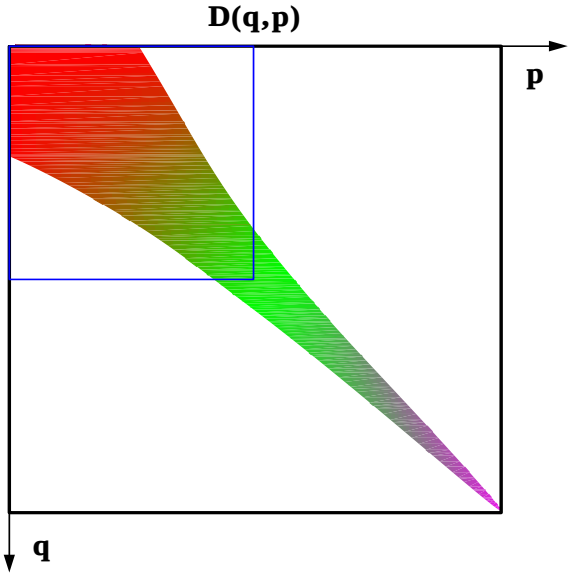

Figure 3. Structure of the Wilson operator in momentum space and in a smooth gauge.

obtained for the masses are also reported in the Table. The errors have been evaluated with the jackknife method. Fig. 1 illustrates the behavior of the isotriplet mass M_π in the model with two flavors. This mass is expected to vanish for $m = 0$ and chiral perturbation theory predicts an $m^{2/3}$ dependence on m (see Eq. 9). To test this functional dependence we performed two different fits. First the pion masses were fitted as

$$\frac{M_\pi}{g} = A + B\left(\frac{m}{g}\right)^{2/3} \tag{13}$$

using only the highest four quark masses for which $24 \times M_\pi > 4$. The results of the fit $A = -0.001(65)$ and $B = 2.10(14)$ confirm that Neuberger's fermions preserve chiral symmetry and give values of B in very good agreement with the theoretical prediction. The dashed line in Fig. 1 is the result of the fit. We then fitted the pion mass as

$$\frac{M_\pi}{g} = B\left(\frac{m}{g}\right)^{\delta} \tag{14}$$

obtaining $B = 2.10(17)$ and $\delta = 0.67(6)$ in perfect agreement with the expected functional dependence. Equally gratifying is the comparison of the value of the fermion mass m in the Lagrangian with the value m^{AWI} that can be extracted from the axial Ward identity Eq. 6.

In the Table we also report results for the singlet mass M_η versus $m^{4/3}$, always for $N_f = 2$. The singlet meson propagator is given by the difference of the connected and disconnected terms in the correlator and, because of the cancellations, the errors are larger than in the triplet case. The numerical results are, however, consistent with the theoretical prediction of Eq. 9.

3. Approximation in the Fourier Space

The long range physical properties of the Schwinger Model should be determined by the eigenstates of D with eigenvalues in the neighborhood of $\lambda = m$ (i.e. the eigenstates of V with eigenvalue λ_V closest to -1), since these are the states with are expected to go over the physical states of the continuum in the limit $a \to 0$. This suggests that it should be possible to reconstruct the physical observables from these states alone.

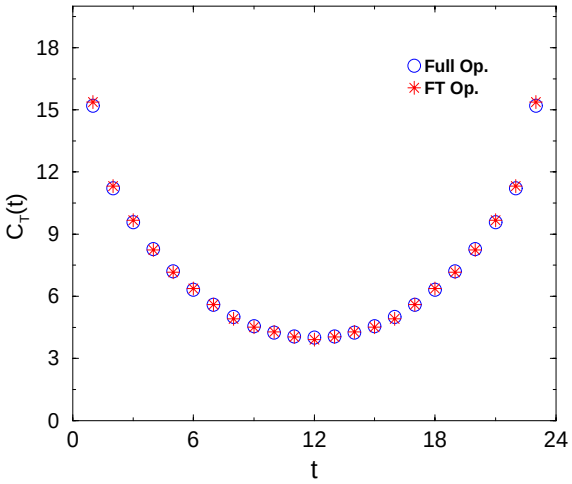

Figure 4. Comparison of the V_2-triplet correlation function computed with the full operator and the Fourier approximation on a configuration with $Q = 0$.

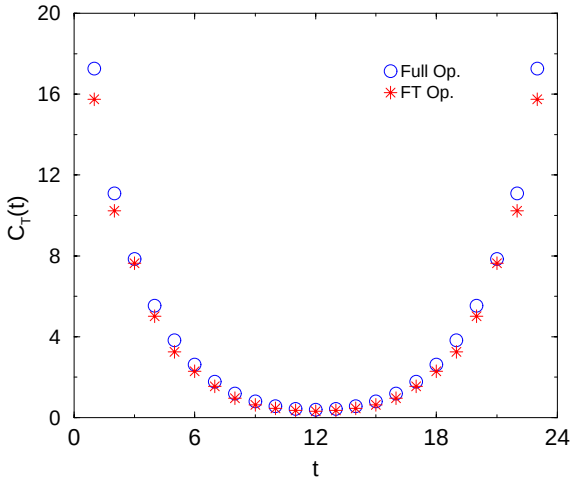

Figure 5. Comparison of the V_2-triplet correlation function computed with the full operator and the Fourier approximation on a configuration with $Q = 4$.

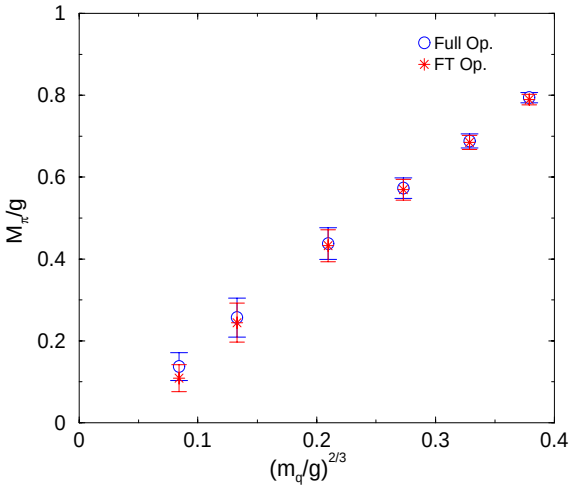

Figure 6. M_π/g vs $(m/g)^{2/3}$ for the full operator (circles,blue) and the Fourier approximation (stars,red) for $N_f = 2$.

Here we would like to make the point that the overlap formulation is particularly well suited for the implementation of the above approximation, since the unitarity of V provides, in some sense, a constraint on the form of the approximation itself. Of course, one must be careful in attempting any approximation based on neglecting the short-wavelength part of the spectrum, even if the corresponding states are largely lattice artifacts, since one knows that in quantum field theory the infrared and ultraviolet components of the spectrum are subtly related. Thus, the chiral eigenstates with $\lambda_V = -1$ ("zero modes"), which V exhibits in presence of a gauge field with nontrivial topology, find their counterpart in states with opposite chirality and $\lambda_V = 1$.

Here too, however, the special features of the overlap formulation come to the rescue, since, as we will show, both the presence of zero modes and the correspondence between $\lambda_V = -1$ and $\lambda_V = 1$ eigenstates of opposite chirality is preserved, as we found in our study, by the projection over a subset of physical states.

One possible scheme of approximation which is computationally very convenient consists of performing a projection over states of low momentum in Fourier space, after gauge fixing to a smooth gauge field configuration[2]. In a smooth gauge, because of the suppression of short-wavelength fluctuations due to asymptotic freedom, one expects the structure of the Wilson operator to become more and more diagonal in momentum space for increasing momenta. This notion is schematically illustrated in Fig. 3 and also underlies the technique of Fourier acceleration for the calculation of quark propagators [7]. Accordingly, we implemented the following approximation. For each configuration we factored out the topology, if any, as described in [2] and fixed the Landau gauge on the resulting configuration by demanding that the function

$$G = \sum_{x,\mu} \mathrm{Re}[U_\mu(x) + U_\mu(x - a\hat{\mu})] \qquad (15)$$

be maximal. A relaxation procedure produces several local maxima (Gribov copies). Among all these configurations, we selected the one that produced the maximum for G, subject to the further constraint that for all x and μ $\mathrm{Re}U_\mu(x) \geq 0.5$.

[2] A similar but gauge invariant procedure is described in [2] which, however, turns out to be numerically more expensive.

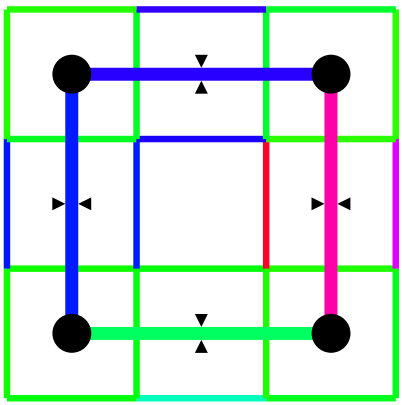

Figure 7. Sketch of the blocking procedure.

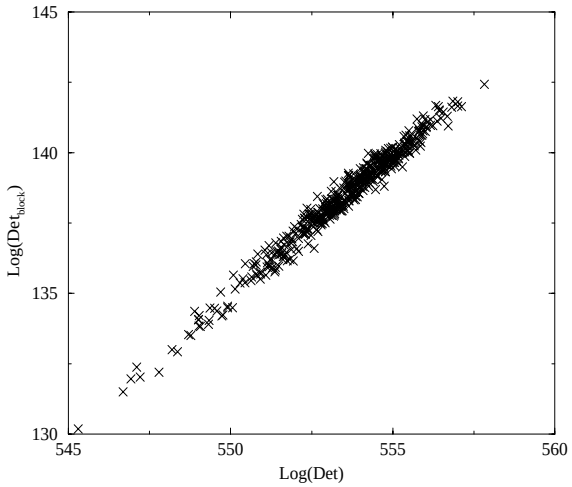

Figure 8. Det(D) on the blocked lattice versus Det(D) on the full lattice.

Eventually the gauge transformation obtained was applied to the original configuration.

Once the gauge has been fixed, the vector space on which the fermion matrix D acts is divided into two parts: a long range (LR) sector spanned by the vectors of the Fourier basis $|p_i\rangle$ $(i = 1, \dots n)$ with $p_i^2 < p_\Lambda^2$ and its complementary short range (SR) subspace. In the LR sector the matrix elements of the Wilson operator are computed and Neuberger's operator is obtained with the unitarity projection in Eq. (2) and inverted. In the SR subspace the propagator is approximated by its free form. The approximated operator is γ_5-Hermitian and it satisfies the GW relation.

In Figs. 4 and (5) we compare the triplet meson correlation functions $C_T(t)$ obtained with the full Neuberger operator and with the approximated one for a configuration with trivial topology and for one with the topological charge $Q = 4$. In Fig. (6) the triplet meson masses for the full solution and the Fourier approximation are reported. The LR subspace used is 1/4 of the full space. It is interesting to note that the approximated solution can be improved if used as preconditioning of the standard algorithms.

4. Multi-Grid Approximation for the Determinant

In the spirit of the long range approximation, another possibility that can be explored is the coarse graining of the gauge field [8]. Starting from an arbitrary gauge configuration on an $N \times N$ lattice, we apply the blocking procedure sketched in Fig. 7 to obtain a gauge configuration on an $\frac{N}{2} \times \frac{N}{2}$ lattice, which carries all the relevant long range features of the large lattice.

The original lattice is divided into $\frac{N}{2} \times \frac{N}{2}$ blocks of 2^2 sites. Each block, after the local Landau gauge is imposed, corresponds to a site of the coarse lattice. The remaining links are averaged as in Fig. 7 to give the corresponding links of the coarse lattice.

The absence of additive mass renormalization simplifies the definition of the Neuberger operator on the coarse lattice because no fine tuning of the mass parameter is needed. We calculated the fermion determinant on the blocked lattice and compared it to the one of the full lattice as shown in Fig. 8.

We incorporated the blocked determinant in the averages of the correlation functions. We compare these results with those obtained with the determinant of the full operator. For the pion

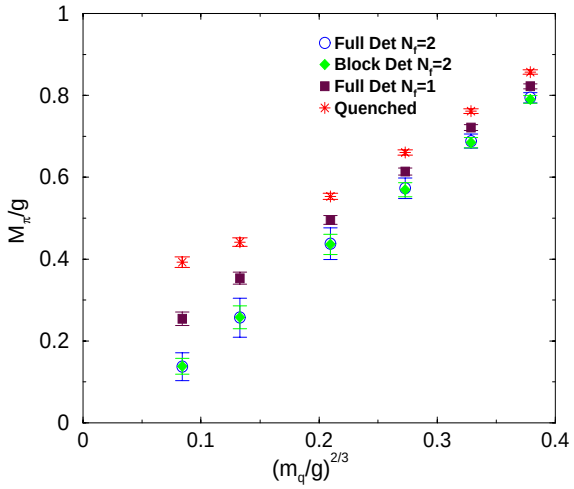

Figure 9. M_π/g vs $(m/g)^{2/3}$ quenched (stars,red), $N_f = 1$ (squares,violet) and $N_f = 2$ (circles,blue) with the full determinant and $N_f = 2$ (diamonds,green) with the blocked determinant.

masses the agreement is remarkable (see Fig. 9). We did the same for the massive Schwinger boson and the results are reported in the Table. Also in this case, even if the observables are more noisy, the agreement between the results is remarkable.

The application of these ideas to speed up QCD simulations with Neuberger fermions is in progress.

REFERENCES

1. H. Neuberger, Phys. Lett. B417 (1998) 141; H. Neuberger, Phys. Lett. B427 (1998) 353.
2. L. Giusti, C. Hoelbling, C. Rebbi, in preparation.
3. P. H. Ginsparg, K. G. Wilson, Phys. Rev. D25 (1982) 2649.
4. M. Lüscher, Phys. Lett. B428 (1998) 342.
5. C. Gattringer, I. Hip, C. B. Lang, Phys. Lett. B466 (1999) 287.
6. C. B. Lang, T. K. Pany, Nucl. Phys. B513 (1998) 645; F. Farchioni et al, Nucl. Phys. B549 (1999) 364.
7. G. Katz et al., Phys. Rev. D37 (1988) 1589.
8. R. Brower, R. Edwards, C. Rebbi, E. Vicari, Nucl. Phys. B336 (1991) 689.